

Synergies between *Euclid*, *Roman* and *JWST* Could Reveal Quasars at up to $z \sim 15$

MUHAMMAD A. LATIF¹ AND DANIEL J. WHALEN²

¹*Physics Department, College of Science, United Arab Emirates University, PO Box 15551, Al-Ain, UAE (latifne@gmail.com)*

²*Institute of Cosmology and Gravitation, Portsmouth University, Dennis Sciama Building, Portsmouth PO1 3FX*

ABSTRACT

Although supermassive black holes (SMBHs) are found at the centers of most galaxies today, over 300 have now been discovered at $z > 6$, including a $4 \times 10^7 M_{\odot}$ BH in **UHZ1 at $z = 10.1$** and an $8 \times 10^7 M_{\odot}$ BH in **GHZ9 at $z = 10.4$** . They are thought to form when $10^4 - 10^5 M_{\odot}$ primordial stars die as direct-collapse black holes (DCBHs) at $z \sim 20 - 25$. While studies have shown that DCBHs should be visible at birth at $z \gtrsim 20$ in the near infrared (NIR) to the *James Webb Space Telescope (JWST)*, none have considered SMBH detections at later stages growth down to $z \sim 6 - 7$. Here, we present continuum NIR luminosities for a quasar like ULAS J1120+0641, a $1.35 \times 10^9 M_{\odot}$ BH at $z = 7.1$, from a cosmological simulation for *Euclid*, *Roman Space Telescope (RST)* and *JWST* bands from $z = 6 - 15$. We find that ***Euclid* and *RST* could detect such BHs**, including others like UHZ1 and GHZ9, at much earlier stages of evolution, out to $z \sim 14 - 15$, and that their redshifts could be confirmed spectroscopically with *JWST*. Synergies between these three telescopes could thus reveal the numbers of quasars at much higher redshifts and discriminate between their formation channels because *Euclid* and *RST* can capture large numbers of them in wide-field surveys for further study by *JWST*.

Keywords: quasars: supermassive black holes — black hole physics — early universe — dark ages, reionization, first stars — galaxies: formation — galaxies: high-redshift

1. INTRODUCTION

Quasars at $z > 6$ were first detected in the *Sloan Digital Sky Survey* over twenty years ago (Fan et al. 2003). Since then, their numbers have risen to over 300, with 13 at $z > 7$ (Mortlock et al. 2011; Bañados et al. 2018; Yang et al. 2020; Wang et al. 2021). A new class of active galactic nuclei (AGNs) has now been found at even higher redshifts, such as a $4 \times 10^7 M_{\odot}$ BH in **UHZ1 at $z = 10.1$** (Castellano et al. 2023a; Bogdán et al. 2023; Goulding et al. 2023) and an $8 \times 10^7 M_{\odot}$ BH in **GHZ9 at $z = 10.4$** (Atek et al. 2023; Castellano et al. 2023b; Kovács et al. 2024). In principle, low-mass Population III (Pop III) stars could be the seeds of these quasars if their BHs accrete continuously at the Eddington limit or grow by super-Eddington accretion (Volonteri et al. 2015; Inayoshi et al. 2016; Lupi et al. 2024). However, this scenario is problematic because Pop III BHs are born in low densities that preclude rapid initial growth (e.g., Kitayama et al. 2004; Whalen et al. 2004; Latif et al. 2022a) and they can be ejected from their host halos during collapse (Whalen & Fryer 2012). When they do accrete, they drive gas out of their halos because of their shallow gravitational potential wells, so

they are restricted to fairly low duty cycles (Smith et al. 2018).

Consequently, it is generally thought that the $z > 6$ quasars grew from DCBHs that form and then rapidly grow in the low-shear environments of rare, massive halos fed by strong accretion flows (Tenneti et al. 2018; Smidt et al. 2018; Lupi et al. 2021; Valentini et al. 2021). The highly supersonic turbulence in these unusual halos produces supermassive stars (SMSs; Hosokawa et al. 2013; Woods et al. 2017; Haemmerlé et al. 2018; Woods et al. 2021; Herrington et al. 2023; Nandal et al. 2024b) without any need for exotic environments (or even atomic cooling, as had been supposed for nearly 20 years; Latif et al. 2022b). DCBHs grow at much higher rates than Pop III BHs because Bondi-Hoyle accretion rates scale as M_{BH}^2 , and they form in much higher densities (e.g., Patrick et al. 2023) in more massive halos that retain gas even when it is photoionized by X-rays (Woods et al. 2019; Latif et al. 2021). SMSs are also probably required to explain the large nitrogen excesses in GN-z11 (Bunker et al. 2023; Senchyna et al. 2024), CEERS 1019 (Larson et al. 2023), and GS 3073 (Ji et al. 2024), high-redshift galaxies at $z \sim 5.5 - 10.5$ (Nagele et al. 2023a; Nandal et al. 2024a, 2025).

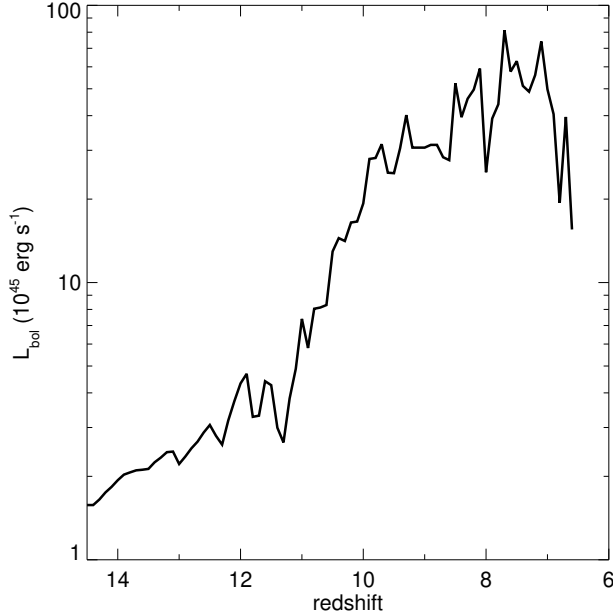


Figure 1. Bolometric luminosities, L_{bol} , for the quasar as a function of redshift from Smidt et al. (2018).

SMSs can be detected in the NIR at $z \sim 8 - 14$ (Surace et al. 2018, 2019; Vikaeus et al. 2022; Nagele et al. 2023b) and DCBHs can be found at $z \gtrsim 20$ by *JWST* (Natarajan et al. 2017; Barrow et al. 2018; Whalen et al. 2020b) and at $z \sim 8 - 10$ by the Square Kilometer Array (SKA) and next-generation Very Large Array (ngVLA; Whalen et al. 2020a, 2021). Quasars like ULAS J1120+0641, a $1.35 \times 10^9 M_{\odot}$ BH at $z = 7.1$ that is typical of $z \sim 6 - 7$ SMBHs, can be detected at much earlier stages of evolution ($z \sim 14 - 15$) at 0.1 - 10 GHz, but only in blind surveys that may not yield many objects because of these telescopes' small fields of view (Whalen et al. 2023; Latif et al. 2024a,b, 2025; Latif & Whalen 2025). However, *Euclid* and *RST* could in principle photometrically identify much larger numbers of quasars at $z > 6 - 7$ because of their large survey areas. Once found, their properties and redshifts could be determined spectroscopically by *JWST*. Observations of quasars at earlier stages of evolution at $z > 7$ are clearly needed to determine their numbers and probe their formation pathways. We have calculated NIR luminosities for a quasar like J1120 at earlier stages of evolution, $z = 6 - 15$, to determine at what redshifts it could be found by *Euclid*, *RST*, and *JWST*. In Section 2 we describe our NIR AB magnitude estimates. We discuss AB mag limits for the quasar in redshift for all three telescopes in Section 3.

2. NUMERICAL METHOD

We calculate NIR magnitudes by normalizing theoretical spectra for BH accretion disks to bolometric lu-

minosities from the quasar similar to J1120 in the cosmological simulation by Smidt et al. (2018), which uses radiation hydrodynamics to model X-ray feedback by the SMBH. We then cosmologically dim and redshift these spectra and convolve them with *Euclid*, *RST*, and *JWST* filter functions to obtain AB magnitudes. We show bolometric luminosities, L_{bol} , for the quasar from $z = 6 - 14.5$ in Figure 1. Over this range in redshift the accretion rates vary from $\sim 0.2 - 0.8 \dot{M}_{\text{Edd}}$, at which the disk is expected to be thin, Compton-thick, and radiatively efficient. We therefore adopt the theoretical spectrum for such disks used by Yue et al. (2013), in which the luminosity is the sum of three components,

$$L_{\nu} = L_{\nu}^{\text{MBB}} + L_{\nu}^{\text{PL}} + L_{\nu}^{\text{refl}}, \quad (1)$$

a multicolor blackbody part due to the range of temperatures across the disk, a power-law component from the surrounding hot corona, and a reflection component, respectively. We omit the contribution due to reflection because it is at most 10% of the entire spectrum and is at energies well above those redshifted into the NIR today.

The temperature of the disk is highest at its center, where

$$T_{\text{max}} = \left(\frac{M_{\text{BH}}}{M_{\odot}} \right)^{-0.25} \text{ keV}, \quad (2)$$

and decreases at larger radii (Makishima et al. 2000; Salvaterra et al. 2005). This approximation is valid if the central engine is a Schwarzschild BH, the innermost radius is about five times the Schwarzschild radius and the accretion is at or near the Eddington limit. The spectral luminosity is then

$$L_{\nu}^{\text{MBB}} = L_{\text{MBB}} \int_0^{T_{\text{max}}} B_{\nu}(T) \left(\frac{T}{T_{\text{max}}} \right)^{-11/3} \frac{dT}{T_{\text{max}}}, \quad (3)$$

where $B_{\nu}(T)$ is the emission spectrum of a blackbody with temperature T and L_{MBB} is a normalization factor.

As in Yue et al. (2013), we parametrize the emission spectrum of the hot corona as a power law with an exponential cutoff:

$$L_{\nu}^{\text{PL}} = L_{\text{PL}} \nu^{\alpha_s} \exp(-h\nu/E_{\text{cut}}), \quad (4)$$

where we set $\alpha_s = 1$, $E_{\text{cut}} = 300$ keV (Sazonov et al. 2004), and L_{PL} is a normalization factor. As in Salvaterra et al. (2005) and Yue et al. (2013), we truncate the power law below the peak of the disk component, at $\sim 3 T_{\text{max}}$.

We estimate normalization factors L_{MBB} and L_{PL} by setting

$$\int (L_{\nu}^{\text{MBB}} + L_{\nu}^{\text{PL}}) d\nu = L_{\text{bol}}. \quad (5)$$

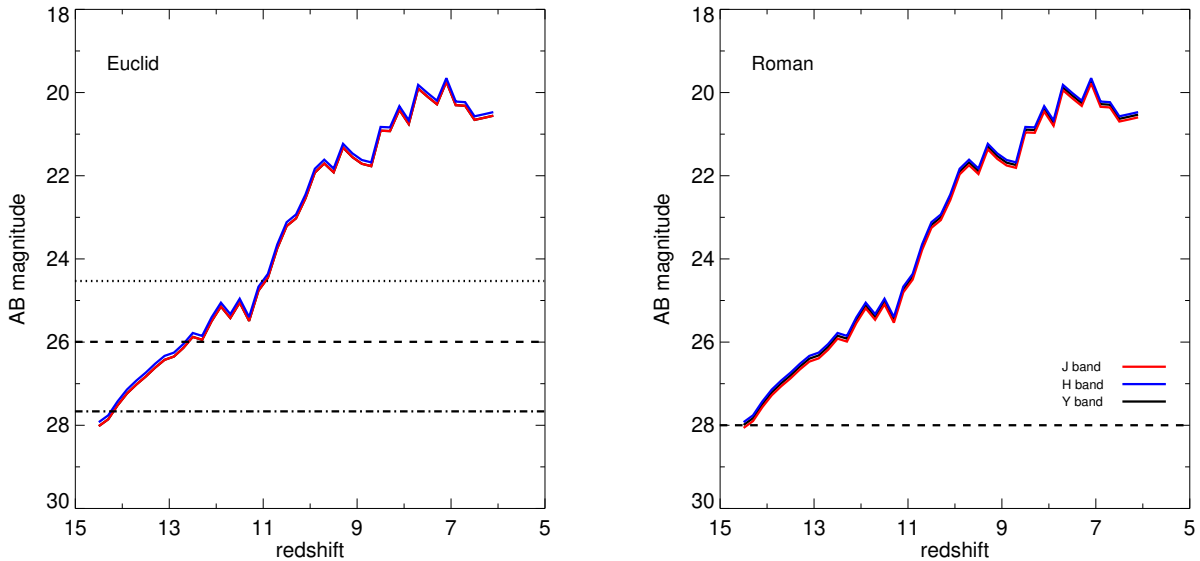


Figure 2. NIR AB magnitudes for the quasar from $z = 6 - 15$. Left: *Euclid* H and J bands. The horizontal dotted, dashed and dot-dash lines are *Euclid* AB magnitude limits for the Wide, Deep and Ultra Deep Surveys, respectively. Right: AB magnitudes in the *RST* H , J and Y bands. The horizontal dashed line is the AB mag limit for the High Latitude Spectroscopic Survey.

Following [Yue et al. \(2013\)](#), this then leads to

$$L_{\text{MBB}} = 0.5 L_{\text{bol}} / \int L_{\nu}^{\text{MBB}} d\nu \quad (6)$$

and

$$L_{\text{PL}} = 0.5 L_{\text{bol}} / \int L_{\nu}^{\text{PL}} d\nu. \quad (7)$$

3. RESULTS AND DISCUSSION

We show AB magnitudes for the quasar at $z = 6 - 14.5$ in the *Euclid* H and J bands and the *RST* H , J and Y bands in Figure 2. We superimpose detection limits for the 14000 deg^2 *Euclid* Wide Survey (WS, 24.5 AB mag; [Euclid Collaboration et al. 2025](#)), the 50 deg^2 Deep Survey (DS; 26.0 AB mag), the $\sim 1 \text{ deg}^2$ Ultra Deep Survey (EUDS; 27.7 AB mag) on the left panel and for the 2000 deg^2 *RST* High Latitude Spectroscopic Survey (HLSS, 28 AB mag; [Wang et al. 2022](#)) on the right panel. The *Euclid* WS could photometrically detect a quasar like J1120 at redshifts up to $z \sim 11$ while the DS and EUDS could detect them out to $z \sim 13$ and $z \sim 14$, respectively, when the BH only has a mass of $\sim 10^6 M_{\odot}$ and an accretion rate of $\sim 0.8 \dot{M}_{\text{Edd}}$ (see Figures 2 and 3 of [Smidt et al. 2018](#)). These are effectively the upper limits in z for detection by *Euclid* because photons redshifted into the H and Y band filters from earlier times would be blueward of the Lyman limit in the rest frame and be resonantly scattered or absorbed by the neutral IGM.

In contrast, *RST* could detect this quasar at $z \lesssim 14.5$ in the H , J and Y filters, making it the observatory of

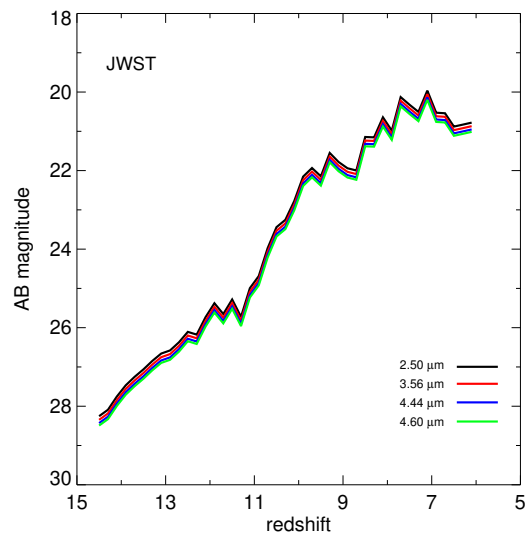


Figure 3. NIR AB magnitudes for the quasar from $z = 6 - 15$ in the *JWST* 2.50 μm , 3.65 μm , 4.44 μm and 4.60 μm NIRcam bands. The *JWST* NIRcam AB magnitude limit is 32 for these filters, below the scale of the plot.

choice for initial detection of quasars at earlier times because of its high sensitivities and large survey areas. We show AB magnitudes in the 2.50 μm , 3.65 μm , 4.44 μm and 4.60 μm *JWST* NIRcam filters in Figure 3. They are well above NIRcam detection limits (\sim AB mag 32, not visible in the plot), or even NIRSpc limits, ~ 29 at $z \lesssim 15$. *JWST* could thus spectroscopically confirm redshifts of BHs with masses as low as $\sim 10^6 M_{\odot}$ if they accrete at or about the Eddington limit at $z \sim 15$.

Ultimately, *RST* could detect SMBHs out to $z \sim 18$ because its F213 filter extends down to $2.30 \mu\text{m}$, unlike *Euclid*'s *H* band filter, which cuts off at $2.0 \mu\text{m}$ and would limit detections to $z \sim 15.5$. Although the BH we consider drops below *RST*'s detection limit at $z = 14.5$, this does not rule out SMBH detections at higher redshifts because they could form at earlier times and reach similar masses by $z \sim 18$. *RST* also has seven filters as opposed to *Euclid*'s four for better initial redshift cuts for dropouts. Most importantly, *RST* will have unparalleled sensitivity over large survey areas, so it will be the best bet for initial identification of high- z quasars.

Although *RST* will perform slitless spectroscopy at $0.8 - 1.9 \mu\text{m}$, the one hour exposure required to reach AB mag 28 in the *H* band will only produce 10σ continuum sensitivity limits of AB mag 21 and 23 for point sources in the prism and grism, respectively, insufficient for determination of high redshifts. Consequently, both *RST* and *Euclid* will have to rely on efficient photometric techniques such as dropouts or fits of spectral energy distribution templates to the observed photometry with Bayesian methods or neural networks to determine red-

shifts at high z . These fast, efficient techniques will also be required to characterize the sheer numbers of objects that will appear in large surveys.

However, the accuracy of these techniques can fall off at high redshifts, so *JWST* or ground-based extremely large telescopes (ELTs) are needed to spectroscopically confirm redshifts for high- z SMBH candidates found by *RST* and *Euclid*. *JWST* is the best telescope for this purpose, given the (sometimes severe) systematics due to atmospheric transmission associated with the ELTs. SKA and ngVLA could also play an important role by confirming the presence of a BH in these candidates at $z \lesssim 14$, especially at 1 - 10 GHz where flux from the BH dominates synchrotron emission by supernova remnants in the host galaxy (see Figure 2 in Latif et al. 2024b). Exciting new synergies between *Euclid*, *RST* and *JWST* will inaugurate the era of $5 < z < 15$ quasar astronomy in the coming decade.

ACKNOWLEDGMENTS

MAL thanks the UAEU for funding via UPAR grants No. 31S390 and 12S111.

REFERENCES

- Atek, H., et al. 2023, MNRAS, 524, 5486
 Bañados, E., et al. 2018, Nature, 553, 473
 Barrow, K. S. S., Aykutalp, A., & Wise, J. H. 2018, Nature Astronomy, 2, 987
 Bogdán, Á., et al. 2023, Nature Astronomy
 Bunker, A. J., et al. 2023, A&A, 677, A88
 Castellano, M., et al. 2023a, ApJL, 948, L14
 —. 2023b, ApJL, 948, L14
 Euclid Collaboration et al. 2025, A&A, 697, A1
 Fan, X., et al. 2003, AJ, 125, 1649
 Goulding, A. D., et al. 2023, arXiv e-prints, arXiv:2308.02750
 Haemmerlé, L., Woods, T. E., Klessen, R. S., Heger, A., & Whalen, D. J. 2018, MNRAS, 474, 2757
 Herrington, N. P., Whalen, D. J., & Woods, T. E. 2023, MNRAS, 521, 463
 Hosokawa, T., Yorke, H. W., Inayoshi, K., Omukai, K., & Yoshida, N. 2013, ApJ, 778, 178
 Inayoshi, K., Haiman, Z., & Ostriker, J. P. 2016, MNRAS, 459, 3738
 Ji, X., et al. 2024, arXiv e-prints, arXiv:2404.04148
 Kitayama, T., Yoshida, N., Susa, H., & Umemura, M. 2004, ApJ, 613, 631
 Kovács, O. E., et al. 2024, ApJL, 965, L21
 Larson, R. L., et al. 2023, ApJL, 953, L29
 Latif, M. A., Aftab, A., & Whalen, D. J. 2024a, AJ, 167, 251
 Latif, M. A., Aftab, A., Whalen, D. J., & Mezcua, M. 2025, A&A, 694, L14
 Latif, M. A., Khochfar, S., Schleicher, D., & Whalen, D. J. 2021, MNRAS, 508, 1756
 Latif, M. A., Whalen, D., & Khochfar, S. 2022a, ApJ, 925, 28
 Latif, M. A., & Whalen, D. J. 2025, MNRAS, 537, 3448
 Latif, M. A., Whalen, D. J., Khochfar, S., Herrington, N. P., & Woods, T. E. 2022b, Nature, 607, 48
 Latif, M. A., Whalen, D. J., & Mezcua, M. 2024b, MNRAS, 527, L37
 Lupi, A., Haiman, Z., & Volonteri, M. 2021, MNRAS, 503, 5046
 Lupi, A., Quadri, G., Volonteri, M., Colpi, M., & Regan, J. A. 2024, A&A, 686, A256
 Makishima, K., et al. 2000, ApJ, 535, 632
 Mortlock, D. J., et al. 2011, Nature, 474, 616
 Nagele, C., Umeda, H., & Takahashi, K. 2023a, MNRAS, 523, 1629
 Nagele, C., Umeda, H., Takahashi, K., & Maeda, K. 2023b, MNRAS, 520, L72
 Nandal, D., Regan, J. A., Woods, T. E., Farrell, E., Ekström, S., & Meynet, G. 2024a, A&A, 683, A156

- Nandal, D., Whalen, D. J., Latif, M. A., & Heger, A. 2025, arXiv e-prints, arXiv:2502.04435
- Nandal, D., Zwick, L., Whalen, D. J., Mayer, L., Ekström, S., & Meynet, G. 2024b, *A&A*, 689, A351
- Natarajan, P., Pacucci, F., Ferrara, A., Agarwal, B., Ricarte, A., Zackrisson, E., & Cappelluti, N. 2017, *ApJ*, 838, 117
- Patrick, S. J., Whalen, D. J., Latif, M. A., & Elford, J. S. 2023, *MNRAS*, 522, 3795
- Salvaterra, R., Haardt, F., & Ferrara, A. 2005, *MNRAS*, 362, L50
- Sazonov, S. Y., Ostriker, J. P., & Sunyaev, R. A. 2004, *MNRAS*, 347, 144
- Senchyna, P., Plat, A., Stark, D. P., Rudie, G. C., Berg, D., Charlot, S., James, B. L., & Mingozi, M. 2024, *ApJ*, 966, 92
- Smidt, J., Whalen, D. J., Johnson, J. L., Surace, M., & Li, H. 2018, *ApJ*, 865, 126
- Smith, B. D., Regan, J. A., Downes, T. P., Norman, M. L., O’Shea, B. W., & Wise, J. H. 2018, *MNRAS*, 480, 3762
- Surace, M., Zackrisson, E., Whalen, D. J., Hartwig, T., Glover, S. C. O., Woods, T. E., Heger, A., & Glover, S. C. O. 2019, *MNRAS*, 488, 3995
- Surace, M., et al. 2018, *ApJL*, 869, L39
- Tenneti, A., Di Matteo, T., Croft, R., Garcia, T., & Feng, Y. 2018, *MNRAS*, 474, 597
- Valentini, M., Gallerani, S., & Ferrara, A. 2021, *MNRAS*, 507, 1
- Vikaeus, A., Whalen, D. J., & Zackrisson, E. 2022, *ApJL*, 933, L8
- Volonteri, M., Silk, J., & Dubus, G. 2015, *ApJ*, 804, 148
- Wang, F., et al. 2021, *ApJL*, 907, L1
- Wang, Y., et al. 2022, *ApJ*, 928, 1
- Whalen, D., Abel, T., & Norman, M. L. 2004, *ApJ*, 610, 14
- Whalen, D. J., & Fryer, C. L. 2012, *ApJL*, 756, L19
- Whalen, D. J., Latif, M. A., & Mezcua, M. 2023, *ApJ*, 956, 133
- Whalen, D. J., Mezcua, M., Meiksin, A., Hartwig, T., & Latif, M. A. 2020a, *ApJL*, 896, L45
- Whalen, D. J., Mezcua, M., Patrick, S. J., Meiksin, A., & Latif, M. A. 2021, *ApJL*, 922, L39
- Whalen, D. J., Surace, M., Bernhardt, C., Zackrisson, E., Pacucci, F., Ziegler, B., & Hirschmann, M. 2020b, *ApJL*, 897, L16
- Woods, T. E., Heger, A., Whalen, D. J., Haemmerlé, L., & Klessen, R. S. 2017, *ApJL*, 842, L6
- Woods, T. E., Patrick, S., Elford, J. S., Whalen, D. J., & Heger, A. 2021, *ApJ*, 915, 110
- Woods, T. E., et al. 2019, *Publications of the Astronomical Society of Australia*, 36, e027
- Yang, J., et al. 2020, *ApJL*, 897, L14
- Yue, B., Ferrara, A., Salvaterra, R., Xu, Y., & Chen, X. 2013, *MNRAS*, 433, 1556